Dual Notched-Band Crescent Moon Dielectric Resonator Antenna

Mohamed Debab, Amina Bendaoudi, and Zoubir Mahdjoub

***Abstract*— In this article, a dual-band notched ultra-wideband (UWB) dielectric resonator antenna is proposed. The antenna structure consists of Crescent Moon Dielectric Resonator (CMDR) fed by a stepped microstrip monopole printed antenna, partial ground plane, and an I-shaped stub. The Crescent Moon dielectric resonator is placed on the microstrip monopole printed antenna to achieve wide impedance bandwidth, and the I-shaped stub is utilized to improve impedance bandwidth for the WiMAX band. A comprehensive parametric study is carried out using HFSS software to achieve the optimum antenna performance and optimize the bandwidth of the proposed antenna. The entire band is useful with two filtered bands at 5.5 GHz and 6.8 GHz by the creation of notches. The band's rejection, WLAN band (5.2–5.7 GHz), and the downlink frequency band of ITU 7 GHz-band for satellite communication (6.5–7.3 GHz) is realized by inserting G-shaped and C-shaped slots in the ground. The simulation results demonstrate that the proposed CMDR antenna achieves satisfactory UWB performance, with an impedance bandwidth of around 88.7 %, covers the frequency band of 3.2 - 8.3 GHz, excluding a rejection band for the WLAN and ITU 7 GHz band. The CMDR is simulated using HFSS and CST high-frequency simulators.**

***Index Terms*— UWB, Crescent Moon Dielectric Resonator (CMDR), Dual band notched band, C-shaped slot.**

Original Research Paper
DOI: 10.53314/ELS2125011D

I. Introduction

Initially, high permittivity dielectric resonators (DRs) are used as oscillators and filters in microwave circuits. In the last few decades, DR's are only used as energy storage devices rather than radiators. The idea of using DR as an antenna is widely accepted after work done on cylindrical dielectric resonator antenna (DRA) in 1983 [1]. Since dielectric resonator antennas have very low loss, higher efficiency without any conductor loss has ensued DRAs can be excited by different feeding mechanisms with various shapes [2]. Moreover, various types of feeding techniques were utilized to excite DRAs such as using a microstrip feed-line [3], [4] a rectangular waveguide [5], and a coaxial probe [6]. Several techniques have been reported to enhance the bandwidth of DRAs with the use of different configuration shapes, e.g., L-shaped, elliptical-shaped, T-shaped, and stair-shaped [7]–[11]. On the other hand, in the UWB operating frequency band, there exists interference from some narrowband, frequencies. Therefore, certain frequencies in the UWB range need to be rejected leading to a need for band-notched antennas. The main problem of band rejection design is the difficulty of controlling the bandwidth of the notched band in a limited antenna space. Recently, several UWB antennas with band-notched properties were presented where various methods have been used to achieve the band notching. Examples of approaches used are; L-shaped two slots and open-loop resonator [12], U-shaped slots [13], [14], E-shaped slot [15], inverted U-shaped slots and H-shaped slot [16], negative permittivity CSRR [17], and EBG structures [18].

In the present paper, a compact 25×25mm^2 CMDR antenna loaded on a 50Ω microstrip feed line is presented, the antenna can reject two narrow bands by creating narrow slots on the ground plane. The CMDR antenna achieves an impedance bandwidth of 3.2-8.3 GHz with a return loss $|S_{11}| \leq$ -10 dB and presents the decrement gain at 5.5 and 6.8 GHz. This manuscript contains four distinct sections. Section I is an introduction. Section II elaborates the effect geometry and position of the crescent moon dielectric resonator, the design principle with variable frequency band notch characteristics. The radiation pattern and simulation results of return loss with two simulators using CST and HFSS software are presented in Section III. Concluding remarks are presented in Section IV.

II. Antenna Design and Studies

Fig.1 shows the details of the CMDR antenna. The thin monopole antenna is printed on a Rogers RT5880 substrate 25×25 mm^2 whose thickness is 0.878mm, a relative dielectric constant of ε_r = 2.2, and loss tangent of 0.0009. The partial ground plane with a size of 25×8.4mm^2 is applied on the backside of the dielectric substrate. For impedance bandwidth improvement the crescent moon dielectric resonator and I-shaped tuning stub are added for the best matching of the monopole antenna. To create a crescent moon dielectric, the cylindrical dielectric resonator made of Silicon material (relative permittivity of 11.9, and loss tangent tan δ=0.015), with dimensions of R_{DR}=6mm, H_{DR}=14mm. A circular region is cut in the cy-

Manuscript received 7 December 2020. Received in revised form 2 February 2021. Accepted for publication 26 March 2021.

M. Debab is with the Department of Electronics, Faculty of Technology, Hassiba Benbouali, University Chlef 02000, Algeria (e-mail: debab_telecoms2005@hotmail.fr).

A. Bendaoudi is with Laboratory of Electromagnetism, Photonics, and Optronics (LEPO), Djillali liabes, University Sidi Bel Abbes 22000, Algeria (e-mail:aminabendaoudi@yahoo.fr).

Z. Mahdjoub. is with the Laboratory of Electromagnetism, Photonics, and Optronics (LEPO), Djillali liabes, University Sidi Bel Abbes 22000,(e-mail: mahdjoubz@yahoo.com).

lindrical dielectric resonator at position P_{DRC} (P_{RDCx}=9.5mm, P_{RDCy}=9.5mm) with a radius R_{RDC}=5mm. The key innovation in the proposed design is to use the G-shaped and C-shaped slots to achieve dual-notched band characteristics. The band-notched configurations are involved to produce the wanted stop bands with good frequency selectivity and suitable stop bandwidths to eliminate the interference at 5.2–5.7 GHz, and 6.7-7.3 GHz.

A commercial computer simulation tool High-Frequency Structure Simulator (HFSS), is used to design the antenna. The optimized dimensions are presented in Table I.

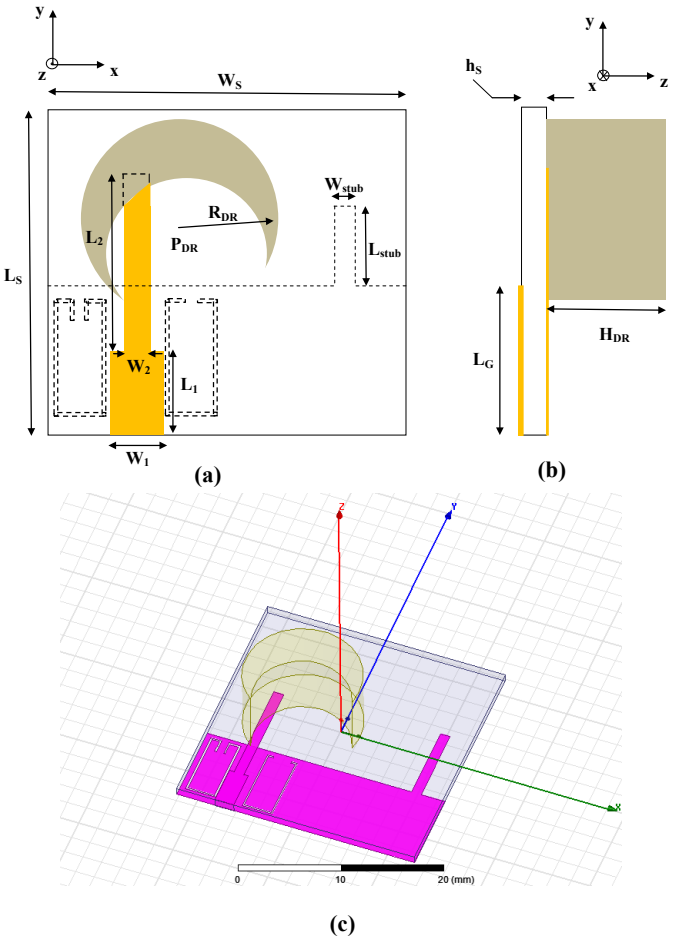

Fig. 1. Geometry of the CMDR antenna (unit: mm): (a) Top view, (b) Side view, (c) 3-D view.

TABLE I. The Parameters of the CMDR Antenna.

parameter	(mm)	parameter	(mm)
W_s	25	H_{DR}	14
L_s	25	P_{DRx}	8.5
h_s	0.878	P_{DRy}	12.5
W_1	2	R_{DRC}	5
L_1	4	P_{DRCx}	9.5
W_2	1	P_{DRCy}	9.5
L_2	11	L_{stub}	8
L_G	8.4	W_{stub}	1
R_{DR}	6		

A. Antenna Without Notches

The design procedure and the simulated reflection coefficients of the CMDR antenna are shown in Fig.2. To increase the bandwidth and move the lower band toward lower frequencies, a CMDR is loaded on the monopole. It can be seen that the monopole antenna loaded with the CMDR, achieves better impedance matching than the basic monopole antenna structure. But the antenna still presents some mismatches at low frequencies band (less than 3.6 GHz). So, to improve this impedance mismatching at low frequencies, an I-shaped tuning stub is added to the partial ground plane, as shown in Fig.2. When the CMDR and I-shaped tuning stub is present, the lower band shifts to 3.3 GHz and the antenna exhibits a sharp resonance dip of $|S_{11}|$ is -22.5dB at 5.2 GHz, and the height of the band shifts to 8.3 GHz. From the simulated results, it can be concluded that the CMDR antenna provides better reflection coefficient performance to cover the WiMAX band.

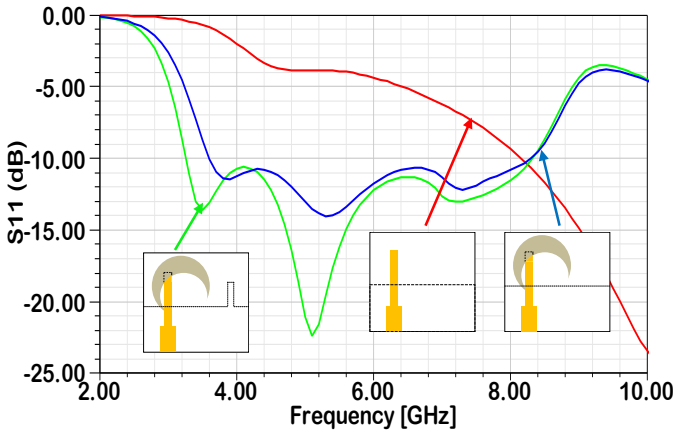

Fig. 2. Simulated $|S_{11}|$ for various antenna structures.

To accomplish an investigation of the characteristics of the CMDR antenna, to obtain the most effective antenna performance, a parametric study is achieved. The commercial software Ansoft HFSS is used for the parametric analysis. Important parameters of the CMDR antenna are investigated by changing each time a parameter while keeping other parameters unchanged.

Fig. 3 shows the effect of the radius R_{DRC} from 1 to 6 mm on antenna performance. It is clear that for $|S_{11}|$ less than -10 dB, the lower edge frequency of the bandwidth is about 3.2 GHz, and the height of the band shifts to 8.3 GHz. When R_{DRC}=5mm. The resulting antenna offers a broad impedance bandwidth of 88.7% for $|S_{11}|$ less than -10 dB.

The effect of the position, P_y on the reflection coefficient of the CMDR antenna is depicted in Fig. 4. From this figure, it is very clear that this parameter influences both the impedance matching and bandwidth of the CMDR antenna. As a result, the best impedance matching is achieved at P_y=12.5 mm.

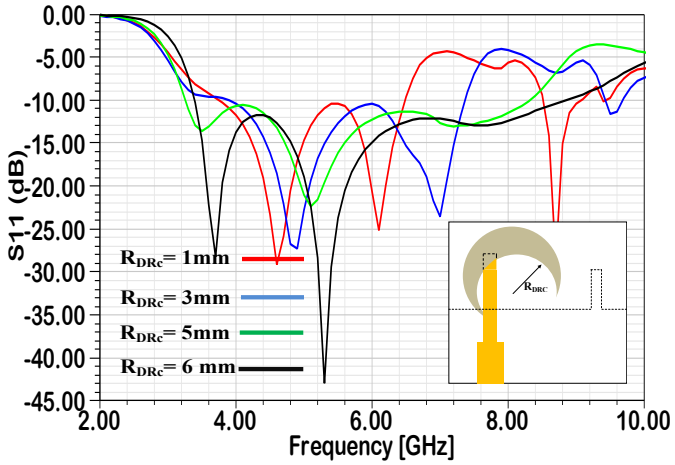

Fig. 3. Simulated $|S_{11}|$ parameters of the CMDR antenna with different values of radius RDRC.

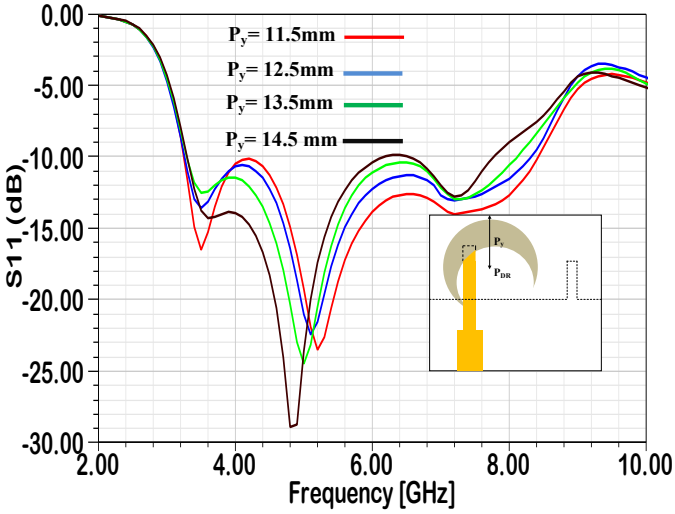

Fig. 4. Simulated $|S_{11}|$ parameters of the CMDR antenna with different positions P_y.

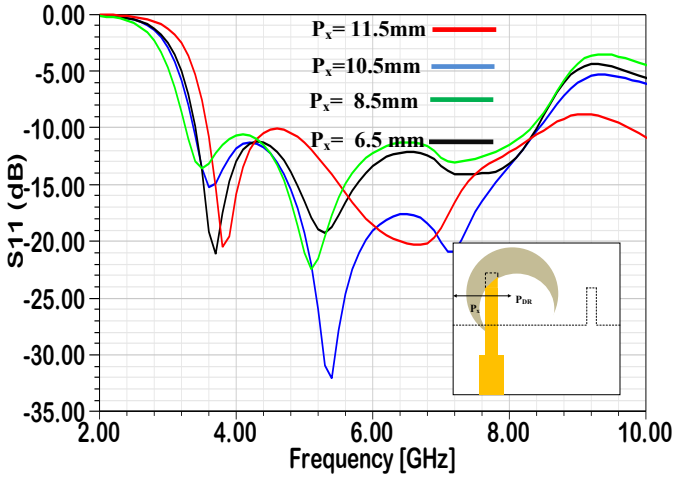

Fig. 5. Simulated $|S_{11}|$ parameters of the CMDR antenna with different positions P_x.

The position P_x has been optimized from 11.5 to 6.5mm to obtain the optimal impedance matching ($|S_{11}| \leq$ -10dB). The comparison of the reflection coefficient versus frequency plot for the different values of the position P_x has been depicted in Fig.5. It can be contemplated that for P_x=8.5 mm, the $|S_{11}|$ is $\leq$ -10dB at the frequency range of 3.2-8.3 GHz.

B. A Configuration of Uwb Antenna with Variable Frequency Band Notch Characteristic

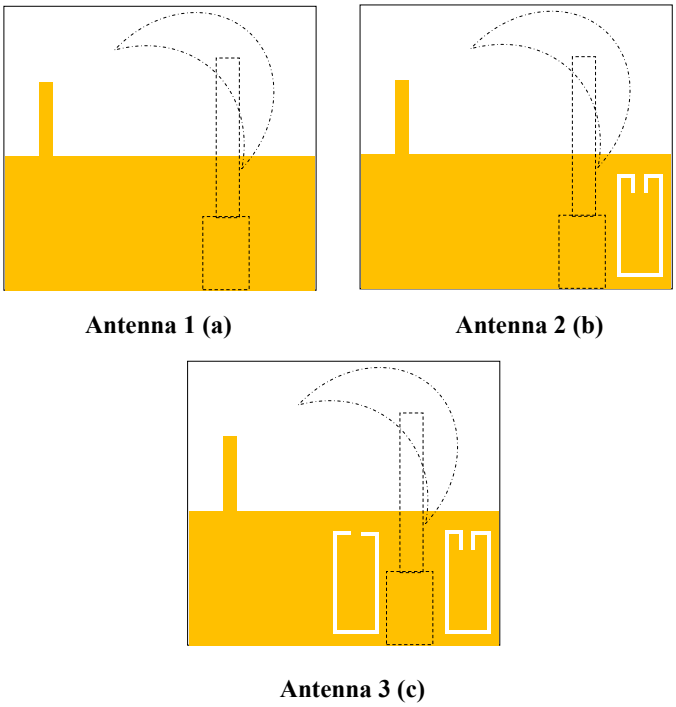

Fig. 6. Evolution of the CMDR antenna: (a) The CMDR antenna, (b) The CMDR antenna with etched G-shaped slot, (c) The CMDR antenna with etched G-shaped and C-shaped slots.

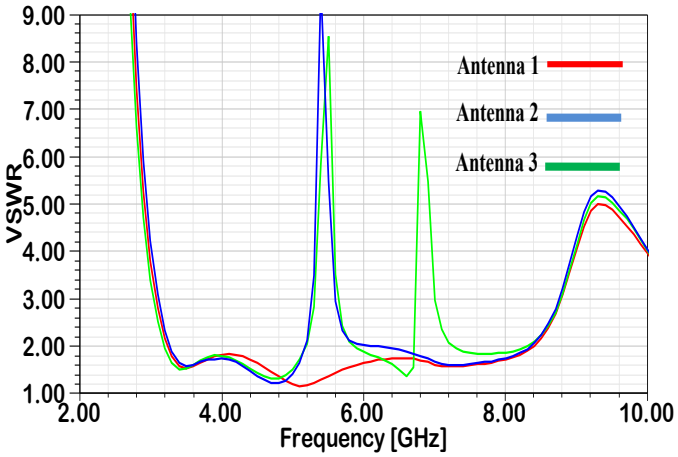

Fig. 7. Simulated *VSWR* of the CMDR antenna with and without slots.

Fig. 6 shows the evolution stages of the proposed design. The antenna is designed with a frequency range of 3.2-8.3 GHz as shown in Fig. 6 (a). By embedded a G-shaped slot on a

ground plane, the band stop function for WLAN is achieved as shown in Fig 6 (b). Dual-band stop characteristics for WLAN band and ITU 7 GHz by etching G-shaped slot and C-shaped slot on the ground plane. The proposed geometry is shown in Fig. 6 (c).

Fig.7 shows the VSWR curves of the evolution of the CMDR antenna. Antenna-2 anticipates the band notch characteristic only at the WLAN frequency band (5.2-5.7 GHz), whereas Antenna 3 shows the band notch characteristics at WLAN (5.2-5.7 GHz) and ITU 7 GHz band (6.7-7.3 GHz).

C. Notched Band for Wlan Band.

The G-shaped slot determines the notched band that rejects the WLAN band, and the designed central frequency of the notch band function is to adjust the length of the slot L_{WLAN} which cuts to approximately half wavelength. Fig. 8 depicts the geometry of the G-shaped slot to create band rejection to avoid the electromagnetic interference between nearby existing WLAN systems and UWB systems. The notched frequency can be assumed as [19]:

$$f_{notch} \approx \frac{c}{2\,L_{WLAN}\sqrt{\frac{\varepsilon_r+1}{2}}} \tag{1}$$

where L_{WLAN} is the total of the G-shaped, ε_r is the dielectric constant of the substrate, and c is the speed of the light. The total length of the slot L_{WLAN} is given by:

$$L_{WLAN} = 2(L_1 + L_2 + L_3) + L_4 = 22mm \tag{2}$$

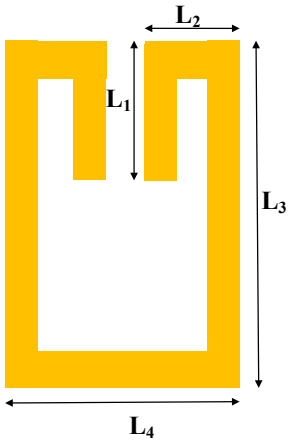

Fig. 8. G-shaped slot dimensions.

Fig. 9 shows the VSWR of the CMDR antenna after adding the C-shaped slot. As observed from the figure a notched band at about 5.5 GHz for the WLAN application is being created. Using equation (1) the theoretical predictions are compared to the total length simulation values L_{WLAN} in Table II. It is found that there are few differences between them.

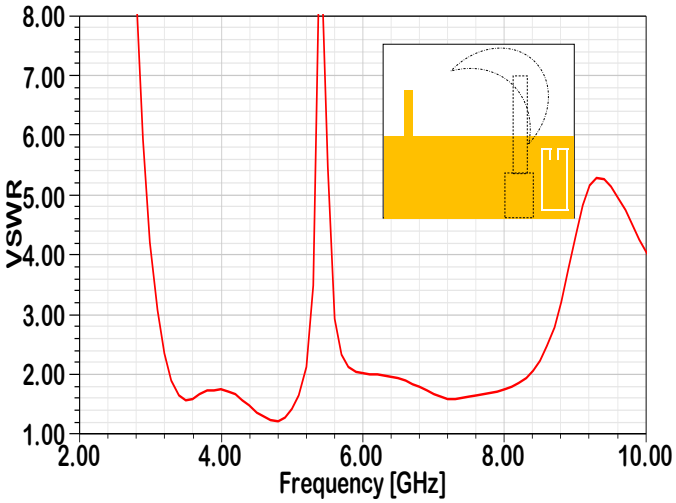

Fig. 9. Simulated *VSWR* of the CMDR antenna with band notch at *WLAN* band.

TABLE II. SIMULATIONS AGAINST THEORETICAL PREDICTION OF WLAN BAND-NOTCHED CMDR ANTENNA.

L_{WLAN} (mm)	Predicted (GHz)	Simulated (GHz)
21.2	5.59	5.70
22	5.39	5.50
22.8	5.20	5.30

D. Notched band for ITU 7 GHz Band

The notched band for ITU 7 GHz band is achieved by etching a C-shaped slot inside the ground plane. Fig.10 depicts the geometry of the C-shaped slot. The appropriate design of the band notch component obtained using the following relation [20]:

$$f_{notch} \approx \frac{c}{2\,L_{ITU}\sqrt{\frac{\varepsilon_r+1}{2}}} \tag{3}$$

Where L_{ITU} is the total length of the C-shaped slot, c is the speed of light, and ε_r is the dielectric permittivity of the substrate. The total length of the slot L_{ITU} is given by:

$$L_{ITU} = 2(L_1 + L_2) + L_3 = 17.8mm \tag{4}$$

From the illustrated Fig.11, a C-shaped slot is used to provide band stop function for ITU 7 GHz Band. It indicated the VSWR characteristics of the proposed geometry. It shows that the antenna provides a sufficiently wide impedance bandwidth (VSWR $\leq$ 2) of 5.1 GHz (3.2-8.3 GHz), and has a frequency notch of about 0.4 GHz (6.7-7.1 GHz) for band rejection of the ITU 7 GHz band. The L_{ITU} length simulation values are compared to the theoretical prediction in Table III. Note that the resonant frequency calculated using equation (3) is in good agreement with simulated notch frequency.

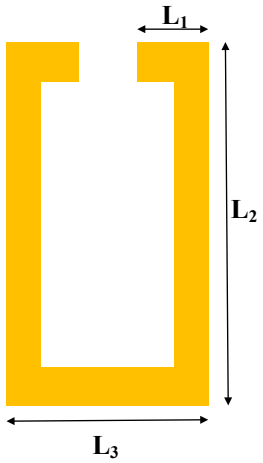

Fig. 10. C-shaped slot dimensions.

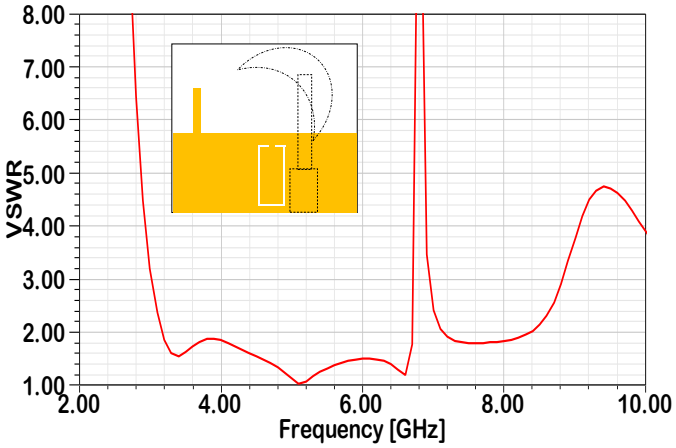

Fig. 11. Simulated *VSWR* of the CMDR antenna with band notch at *ITU* 7 GHz band.

TABLE III. Simulations against Theoretical Prediction of ITU 7 Ghz Band-Notched CMDR Antenna.

L_{ITU} (mm)	Predicted (GHz)	Simulated (GHz)
17.8	6.66	6.80
18.2	6.51	6.60
18.8	6.30	6.50

E. Parametric Study

To study the analysis and effect of various parameters on the bandwidth of notch bands, one parameter at a time is varied. The length L_{WLAN} and L_{ITU} of G-shaped and C-shaped slots are varied and its variation on VSWR is plotted in Fig. 12 and Fig. 13, respectively. The effect of the length L_{WLAN} is presented in Fig.12. The center frequency of the notched band decreases from 5.9 to 5.3 GHz as L_{WLAN} increases from 20.4 to 22.8mm. The figure indicates that any change in the length of the L_{WLAN} does not have any significant influence on the other notched frequency.

Fig.13 plots the VSWR of the CMDR antenna for different values of the length of the C-shaped slot L_{ITU}. It is observed that the center frequency of the band is shifted from 6.5 to 7.3 GHz as the length L_{ITU} changed from 18.8 to 17.2 mm, also observed that the variation in length L_{ITU} of C-shaped negligibly affects the bandwidth of other band notches.

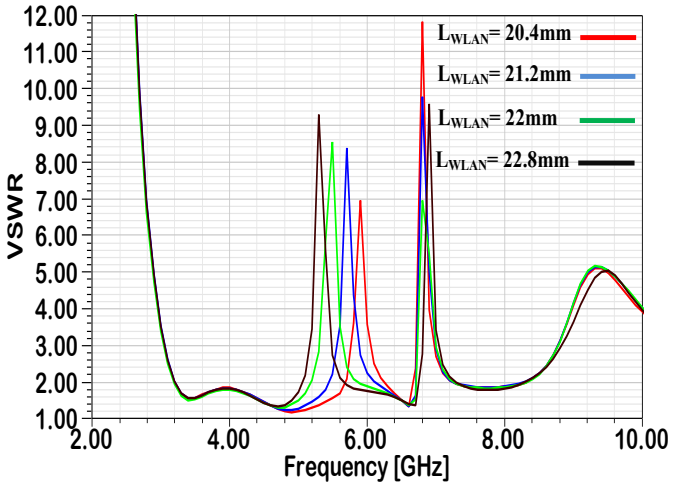

Fig. 12. Simulated *VSWR* of the CMDR antenna with different parameter *LWLAN*.

To understand the phenomena behind the notch band performance, the simulated surface current distribution of CMDR antenna at 5.5 and 6.8 GHz are shown in Fig. 14. It can be observed that at 5.5 GHz the surface current is confined in a G-shaped slot structure, whereas, at 6.8 GHz, the surface current is concentrated in a C-shaped slot. Thus, at these notch frequencies, the antenna will not radiate efficiently.

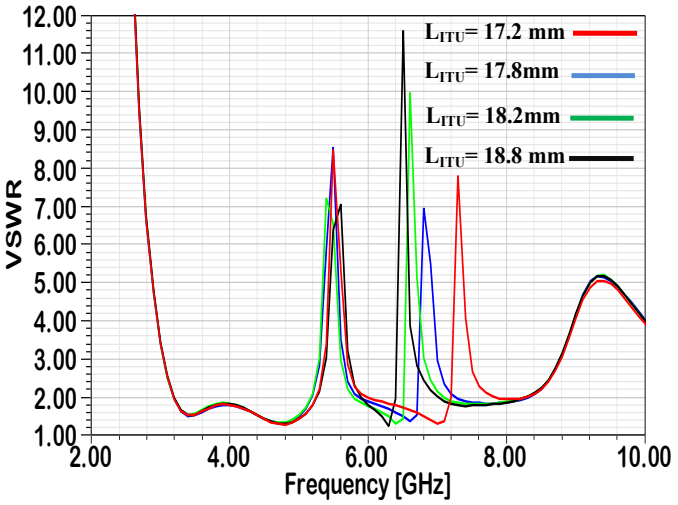

Fig. 13. Simulated VSWR of the CMDR antenna with different parameter *LITU*.

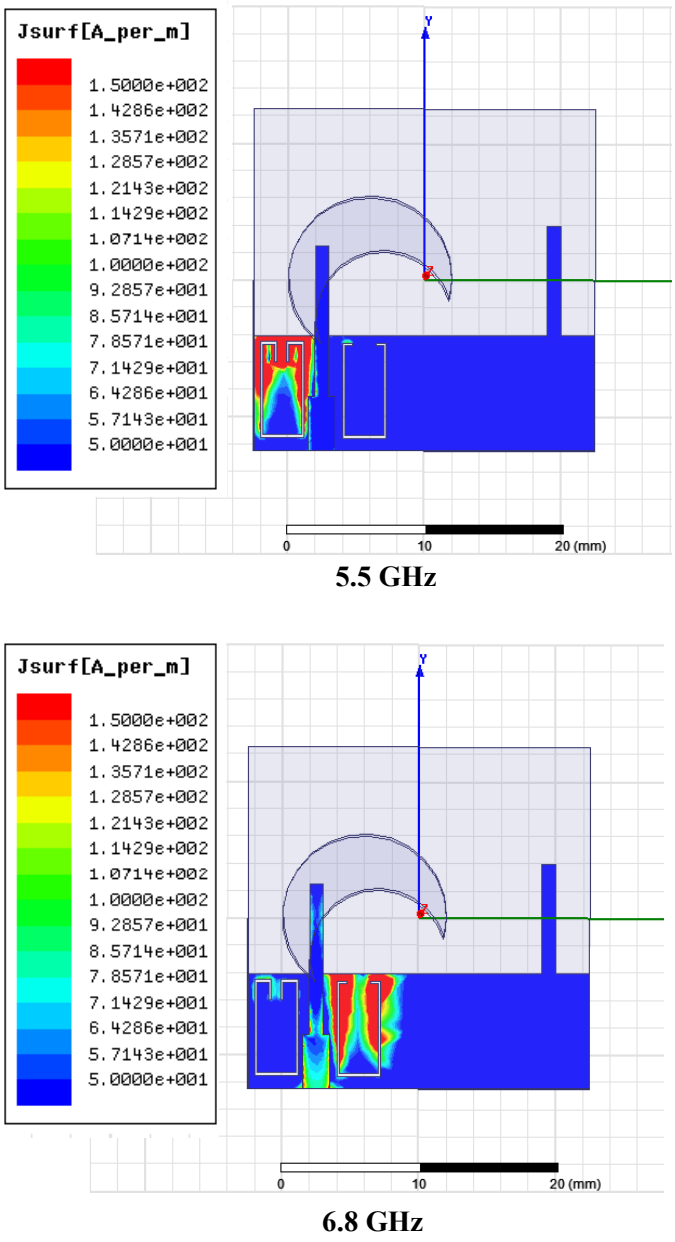

Fig. 14. Surface current distribution of the CMDR antenna at 5.5 and 6.8 GHz.

III. Results

To validate our use of design software HFSS, we designed and simulated the same structure as CST Microwave studio software whose numerical analysis is based on the method of the Finite Integration Technique (FIT). Fig.15 and 16 present the simulated VSWR and the reflection coefficient $|S_{11}|$ obtained by both simulation tools. This result shows a bandwidth of 5.1 GHz, covering frequencies from 3.2 to 8.3 GHz along with two notched bands of 0.5 GHz (5.2-5.7 GHz) and 0.6 GHz (6.7-7.3 GHz). The slight difference between the simulated results of CST and HFSS is due to the different numerical techniques employed by the two software.

The simulation results of radiation patterns at the following frequencies: 4 GHz, 6 GHz, and 8 GHz with two simulators HFSS and CST are shown in Fig. 17. The antenna exhibits an omnidirectional pattern at 4 GHz and it gets distorted and directional as the frequency of operating is increased. At 6 GHz, the radiation pattern is highly directive in the H plane and bidirectional in the E plane. As can be seen that a good agreement is achieved between the two simulators.

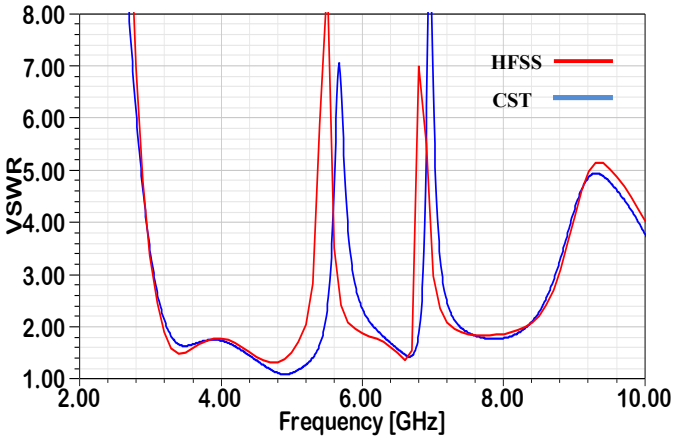

Fig. 15. Simulated *VSWR* of the CMDR antenna using HFSS and CST.

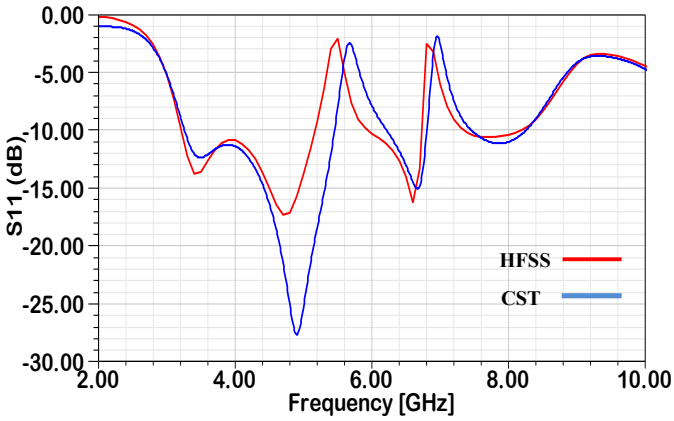

Fig. 16. Simulated $|S11|$ parameters of the CMDR antenna using HFSS and CST.

Fig.18 shows the simulated antenna gain response. The average gain for the dual band-notched antenna in the 3.2-8.3 GHz band is about 3.3dBi, however, at the notched bands 5.5 and 6.8 GHz, the antenna gain drops to about -5 and -2.5 dBi respectively.

The simulated radiation efficiency of the CMDR antenna with and without notch is depicted in Fig. 19. It is seen to have a sharp decrease across the notch band due to the existence of G-shaped and C-shaped slots on the ground plane. The radiation efficiency of the antenna the first notch (5.5 GHz) is 42% and a second notch (6.8 GHz) is 25%.

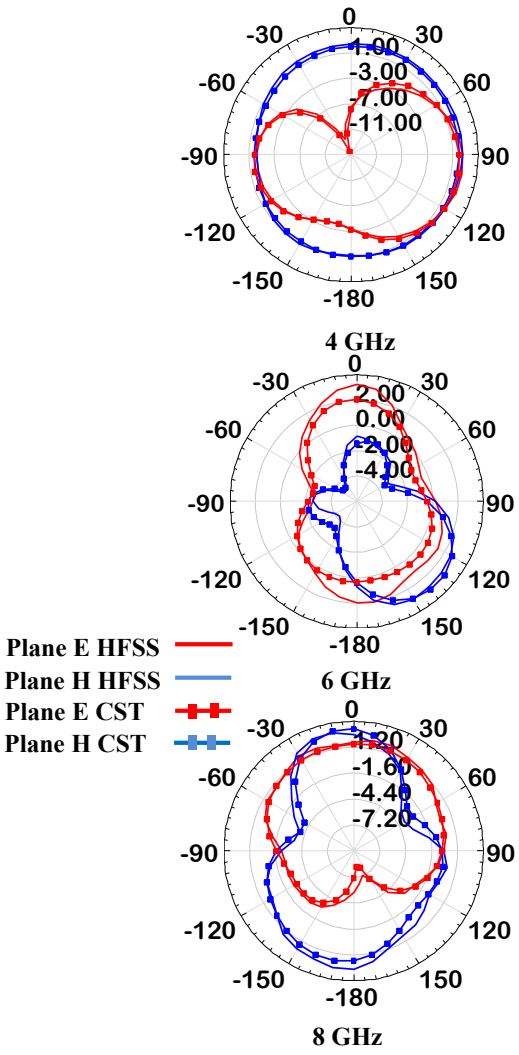

Fig. 17. CST and HFSS simulated directivity patterns in E (y-z) and H (x-z) planes for the CMDR antenna at 4, 6, and 8 GHz.

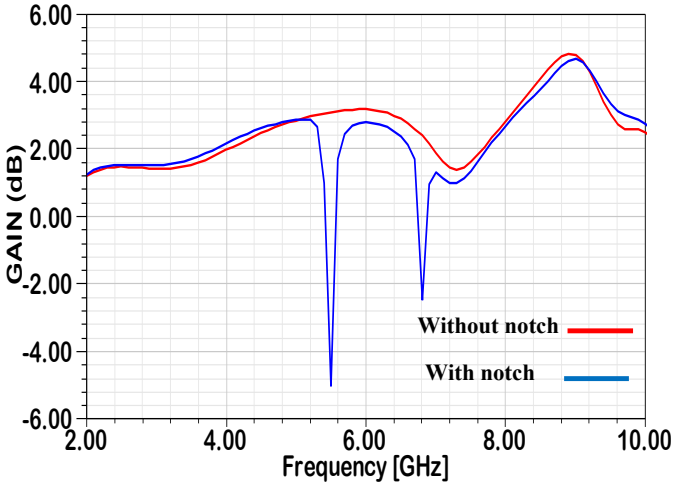

Fig. 18. Simulated peak gain with and without notch of the CMDR antenna.

The comparison of the CMDR antenna with existing antennas has been delineated in Table IV. It can be adorned from Table IV that the CMDR antenna is compact in size in juxtaposition to references [13], [21]–[25] except reference [26]. Though the size of the antenna designed in [26] is compact, this antenna has only a single band notch frequency. Based on the aforementioned discussion, it can be anticipated that the CMDR antenna is novel, compact in size with a new design, and useful for UWB applications with band notched characteristics at WLAN and the downlink frequency band of ITU 7 GHz.

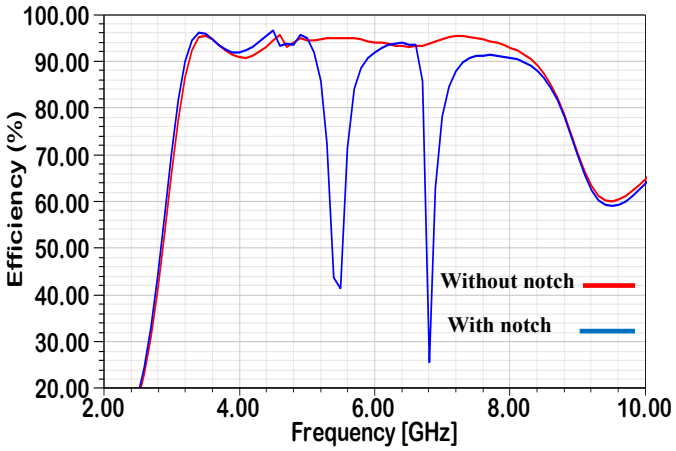

Fig.19. Simulated radiation efficiency with and without notch of the CMDR antenna.

IV. Conclusion

A dual-band notched dielectric resonator antenna is proposed. The UWB is obtained by incorporating a Crescent Moon Dielectric Resonator antenna excited by, a feed line. The I-shaped stub is utilized to improve impedance bandwidth for the WiMAX band. The final dimension of the CMDR antenna is 25×25×14mm^3. The first notch is realized at 5.5 GHz and the second notch is realized at 6.8 GHz by etching G-shaped and C-shaped slots on the ground plane, respectively. The notches prevent interference of 5.2-5.7 GHz (WLAN) and 6.7-7.3 GHz (ITU 7 GHz) communication bands.

The antenna offers UWB with 88.7% (3.2–8.3 GHz) of impedance bandwidth considering $|S_{11}| \leq$-10dB. The simulated results for the antenna VSWR and radiation patterns were provided with the use of HFSS software and were validated by using CST Microwave studio software. The slight difference between the simulated results is due to the different numerical techniques employed by the two software. The simplicity, compact size, low cost, and band rejection make this antenna suitable for UWB applications.

Acknowledgements

This work was supported by the directorate general for scientific research and technological development (DG-RSDT) of Algeria.

TABLE IV. Performance Comparison of the CMDR Antenna with Existing Dielectric Resonator Notched Antenna in Literature.

Ref	Type and shape of the Substrate	Size (mm^2)	VSWR band width range (GHz)	Type, height , and shape of the Dielectric Resonator	Efficiency (%) and Maximum gain at other UWB band (dB)	First rejected frequency band (GHz)	Peak gain of first rejected band (dB)	Second rejected frequency band (GHz)	Peak gain of second rejected band (dB)
[13]	FR4 ε_r=4.4 Rectangular shape	50 x 40	3.3-12	Dupont 943, ε_r=7.4 H_{DR}=6mm, Cylindrical shape	91, 7.6	WiMAX(3.4)	-0.6	---	---
[21]	RT 5880 ε_r=2.2 Rectangular shape	50 x 40	3.1-10.6	---, ε_r=10 H_{DR}=6mm, Rectangular shape	---, 4.5	WiMAX(3.4)	-1	WLAN (5.5)	-4
[22]	RT 3003 ε_r=3 Circular shape	π x $(120)^2$	2-10.7	Tmmi10, ε_r=10 H_{DR}=16.5mm, Inverted Conical shape	---, 8	WLAN(5.5)	-6.5	---	---
[23]	RT 6002 ε_r=2.94 Square shape	30 x30	3.5-10.5	---, ε_r=10.2 H_{DR}=5.08mm A-shape	---, 6	WLAN(5.08)	---	ITU-band Sat. Comm (6.2)	-3.5
[24]	Ground Square shape	90 x 90	3.6-12	Roger 6010, ε_r=10.2 H_{DR}=19mm, Rectangular shape	---, 8	WLAN(5.5)	-2	---	---
[25]	Ground Square shape	50 x 50	3.1-7.25	Roger 3006, ε_r=6.15 H_{DR}=6.5mm Rectangular shape	---, 6.8	WLAN(5.5)	-3	---	---
[26]	RT 3003 ε_r=3 Rectangular shape	11 x 23	3.1-15.25	Eccostock Hik, ε_r= 20 H_{DR}=2mm, S-shape	95, 4.8	WLAN(5.5)	0.9	---	---
Our work	RT 5880 ε_r=2.2 Square shape	25 x 25	3.2-8.3	Silicon, ε_r=11.9 H_{DR}=14mm, Crescent Moon shape	96, 3.6	WLAN(5.5)	-5	ITU-band Sat. Comm (6.8)	-2.5

References

[1] S. A. Long, M. W. Mcallister, and L. C. Shen, "The resonant cylindrical dielectric cavity antenna," *IEEE Transactions. Antennas Propagation*, vol. 31, pp.406-412, May. 1983.

[2] A. Petosa, "Dielectric Resonator Antenna Handbook," *Norwood. A, USA: Artech House*, 2007.

[3] M. A. Saed, and R. Yadla, "Microstrip-fed low profile and compact dielectric resonator antennas," *Progress In Electromagnetics Research*, vol. 56, pp. 151-162, 2006.

[4] A. V. Kumar, V. Hamsakutty, J. Yohannan, and K. T. Mathew, "Microstripline fed cylindrical dielectric resonator antenna with a coplanar parasitic strip," *Progress In Electromagnetics Research*, vol. 60, pp. 143-152, Feb. 2006.

[5] P. Abdulla, and A. Chakraborty, "Rectangular waveguide- fed hemispherical dielectric resonator antenna," *Progress In Electromagnetics Research*, vol. 83, pp. 225-244, Jun. 2008.

[6] S. H. Zainud-Deen, H. A. Malhat, and K. H. Awadalla, "A single-feed cylindrical superquadric dielectric resonator antenna for circular polarization," *Progress In Electromagnetics Research*, vol. 85, pp. 409-424, 2008.

[7] T. A. Denidni, Q. Rao, and A. R. Sebak, "Broadband L-Shaped Dielectric Resonator Antenna," *IEEE Antennas and Wireless Propagation Letters*, vol. 4, pp.453-454, Dec. 2005.

[8] W. Jiang, and W. Q. Che, "A novel UWB antenna with dual notched bands for WIMAX and WLAN applications," *IEEE Antennas and Wireless Propagation Letters*, vol. 11, pp. 293-296, Mar. 2012.

[9] P. V. Bijumon, S. K. Menon, M. N. Suma, B. Lehakumari, M. T. Sebastian, and P. Mohanan, "Broadband elliptical dielectric resonator antenna," *Microwave and Optical Technology Letters*, vol. 48, no. 1, pp. 65-67, Jan. 2006.

[10] Q. Rao, T. A. Denidni, and A. R. Sebak, "Broadband compact stacked t-shaped DRA with equilateral-triangle cross sections," *IEEE Microwave and Wireless Components Letters,* vol.16, no.1, pp. 7-9, Jan. 2006.

[11] R. Chair, A. Kishk , and K. F. Lee, "Wideband stair-shaped dielectric resonator antennas," *IET Microwave, Antennas and Propagation*, vol. 1, no. 2, pp. 299-305, Apr. 2007.

[12] J. W. Wang, J. Y. Pan, X. N. Xiao, and Y. Q. Sun, "A band-notched UWB antenna with L-shaped slots and open-loop resonator," *in Proc IEEE International Conference on Applied Superconductivity and Electromagnetic Devices* , pp. 312–315, Beijing, Oct. 2013.

[13] M. Debab, and Z. Mahdjoub, "Single Band Notched Characteristics UWB Antenna using a Cylindrical Dielectric Resonator and U-shaped Slot," *Journal of Microwaves, Optoelectronics and Electromagnetic Applications*, vol. 17, no. 3, pp. 340-351, Sep. 2018.

[14] R.Yadav, and L. Malviya, "UWB antenna and MIMO antennas with bandwidth, band-notched, and isolation properties for high-speed data rate wireless communication: A review," *International Journal* of *RF and Microwave Computer-Aided Engineering*, vol. 30, no. 2, Feb. 2020.

[15] Y. S. Li, X. D. Yang, C. Y. Liu, and T. Jiang, "Compact CPW-fed ultrawideband antenna with dual band-notched characteristics," *Electronics Letters*, vol. 46, no. 14, pp. 967–968, Jul. 2010.

[16] W. S. Lee, D. Z. Kim, K. J. Kim, and J. W. Yu, "Wide-band planar monopole antennas with dual band-notched characteristics," *IEEE Transactions on Microwave Theory & Techniques*, vol. 54, no. 6, pp. 2800–2806, Jun. 2006.

[17] M. J. Jeong, N. Hussain, H-U. Bong, J. W. Park, K. S. Shin, S. W. Lee, S. Y. Rhee, and N. Kim, "Ultra wideband microstrip patch antenna with quadruple band notch characteristic using negative permittivity unit cells," *Microwave and Optical Technology Letters*, pp. 1-9, Oct. 2019.

[18] R. Sanmugasundaram, S. Natarajan, and R. Rajkumar, "Ultrawideband Notch Antenna with EBG Structures for WiMAX and Satellite Application," *Progress In Electromagnetics Research Letters*, vol. 91, pp. 25–32, Apr. 2020.

[19] G. Srivastava, and A. Mohan, "A planar uwb monopole antenna with dual band notched function," *Microwave and Optical Technology Letters*, vol. 57, no. 1, pp. 99-104, Jan. 2015.

[20] S. Avez, and R. W. Aldhaheri, "A Very Compact and Low Profile UWB Planar Antenna with WLAN Band Rejection," *The Scientific World Journal*, volume 2016, 7 pages, Mar. 2016.

[21] T. A. Denidni, and Z. Weng, "Hybrid ultrawideband dielectric resonator antenna and band-notched designs," *IET Microwaves, Antennas &*

Propagation, vol. 5, no.4, pp. 450-458, Mar. 2011.

[22] M. Niroo-Jazi, and T.A. Denidni, "Experimental Investigations of a Novel Ultrawideband Dielectric Resonator Antenna with Rejection Band Using Hybrid Techniques," *IEEE Antennas and Wireless Propagation Letters,* vol. 11, pp. 492 – 495, May. 2012.

[23] A. Sabouni, and A. Kishk, "Single or multi notch bands applied to microstrip excited ultra-wideband antennas with dielectric resonator antenna case," *Microwave and Optical Technology Letters,* vol. 55, no. 5, pp. 1066-1069, May. 2013.

[24] Y. F. Wang, T. A. Denidni, Q. S. Zeng, and G. Wei, "Band notched UWB rectangular dielectric resonator antenna," *Electronics. Letters.* vol. 50, no. 7, pp. 483–484, Mar. 2014.

[25] M. Debab, and Z. Mahdjoub, "Rectangular Dielectric Resonator Antenna with Single Band Rejection Characteristics," *Journal of Telecommunications and Information Technology*, vol. 1, pp. 76-81, 2019.

[26] P. Chakraborty, J. Debbarma, S. Huda, U. Banerjee, A. Saha, and A. Karmakar, "Ultrawideband Dielectric Resonator Antenna based on Meandered Dielectric Resonator with Band Rejection Characteristics," *International Journal of Science and Research(IJSR)*, vol. 8, no. 7, pp. 1875-1880, Jul. 2019.